2000

Electroporation Dynamics in Biological Cells Subjected to Ultrafast Electrical Pulses: A Numerical Simulation Study

R. P. Joshi
Old Dominion University

K. H. Schoenbach
Old Dominion University

Original Publication Citation

Joshi, R. P., & Schoenbach, K. H. (2000). Electroporation dynamics in biological cells subjected to ultrafast electrical pulses: A numerical simulation study. *Physical Review E, 62*(1), 1025-1033. doi:10.1103/PhysRevE.62.1025

Electroporation dynamics in biological cells subjected to ultrafast electrical pulses: A numerical simulation study

R. P. Joshi and K. H. Schoenbach
Department of Electrical and Computer Engineering, Old Dominion University, Norfolk, Virginia 23529-0246
(Received 11 November 1999)

A model analysis of electroporation dynamics in biological cells has been carried out based on the Smoluchowski equation. Results of the cellular response to short, electric pulses are presented, taking account of the growth and resealing dynamics of transient aqueous pores. It is shown that the application of large voltages alone may not be sufficient to cause irreversible breakdown, if the time duration is too short. Failure to cause irreversible damage at small pulse widths could be attributed to the time inadequacy for pores to grow and expand beyond a critical threshold radius. In agreement with earlier studies, it is shown that irreversible breakdown would lead to the formation of a few large pores, while a large number of smaller pores would appear in the case of reversible breakdown. Finally, a pulse width dependence of the applied voltage for irreversible breakdown has been obtained. It is shown that in the absence of dissipation, the associated energy input necessary reduces with decreasing pulse width to a limiting value. However, with circuit effects taken into account, a local minima in the pulse dependent energy function is predicted, in keeping with previously published experimental reports.

PACS number(s): 87.15.Aa, 87.50.Rr, 87.17.Aa

I. INTRODUCTION

Electroporation is a well known physical process in biological cells [1–3]. It involves rapid structural rearrangement of the membrane in response to an externally applied electric field. The most prominent observable effect is a rapid increase in the electrical conductivity by several orders of magnitude [4]. This is attributed to the formation of aqueous pathways or pores in the lipid bilayer of the membrane that facilitate conduction. The opening of such channels (or more appropriately, transient aqueous pores), also enables the transport of ions and water soluble species both into and out of individual cells. Electroporation can, therefore, be used to initiate large molecular fluxes for the purposes of introducing genetic material into cells and manipulating cells and tissues. Numerous related applications in molecular biology, biotechnology, and medicine are beginning to emerge [5–9].

Electroporation has also been linked to the nonthermal killing of micro-organisms subjected to strong electric fields [10]. For this reason, it offers great potential for decontamination and the elimination of harmful micro-organisms and biohazards. Traditionally, most electroporation studies have focused on relatively low external voltages applied over extended time periods ranging from several tens of microseconds to milliseconds [11]. In a very recent development, work focused on the use of much shorter, high-voltage pulses for initiating electroporation. Electric fields as high as 100 kV/cm were used with pulse durations ranging from nanoseconds to several microseconds. Related field tests on biofouling preventation have also successfully been reported [12,13]. The shift to short electric pulses is guided in part by the development of pulsed power technology. There also appear to be several fundamental advantages to using short electric pulses for cellular manipulation. First, negligible thermal heating of the biological matter can be expected to occur due to the short time duration. Also, much lower energies are required for pulsed inputs, and yet large values of the electric fields and peak powers can be obtained. Since the biological response depends on the magnitude of the applied signal voltage, much more dramatic results can be achieved. The large applied fields would ensure that the quantitative thresholds for almost all of the internal biological mechanisms were adequately exceeded. Consequently, the overall system efficiency is expected to be superior. Next, pulsed fields afford a way by which the time scales can easily be manipulated. This can be used to an advantage by selectively focusing on a desired set of internal processes. For example, by turning off the applied fields relatively quickly, the slower processes (for example, biochemical events) could effectively be inhibited. In theory [14], the time constants for processes ongoing at the membrane, those within the nucleus, and mechanisms occurring within the cell bulk are all expected to be quite different. Hence this scheme appears to offer selective tunability through alterations in the applied pulse width. From the frequency domain standpoint, the magnitude and comparison of the frequency components associated with the forcing function can be made smaller or larger with respect to the internal cellular response times depending on the desired outcome.

The above suggests that electrical pulsed power technology can be an important tool for successfully manipulating the response of biological cells and neutralizing biohazards. Since the application of such high power electric pulses to biological systems is relatively new, not much work has been carried out. In order to fully utilize its potential and optimize the effects, it is quite important to first gain a good understanding of the internal dynamics and electroporation physics. Unfortunately, the precise mechanism of pore formation is not fully understood, though substantial progress has been made over the years. The transient aqueous pore theory suggests a combined role of thermal fluctuations and local electric fields across the membrane [15,16]. Litster [17] and Taupin *et al.* [18] were the first to suggest the role of thermal fluctuations in pore formation. Based on the shape changes necessary, he demonstrated the existence of a threshold pore formation energy. This threshold was associated with the

creation of an edge and elimination of a portion of the surface area. The formation energy depended on the operating temperature. The model was subsequently extended to include electrostatic energy effects [19] and underscored the role of the transmembrane potential $U(r,t)$. Geometric considerations in spherical cells suggest that this potential should predominantly develop over the regions of the two polar caps. Recent fluorescent measurement data [20] has borne this out.

Much of the theoretical work on electroporation has focused on the kinetics and mechanisms for pore formation [7,21–23]. However, the process of pore resealing after the termination of an electric pulse is equally important for practical applications. For instance, this process would control the time duration and amounts of ionic fluid exchanges between cells and external agents. The health of the cells and the likelihood of irreversible breakdown would also be influenced by the pore closing ability. For pulsed power applications, it becomes important to establish a quantitative connection between pore resealing (i.e., reversible breakdown) and the pulse characteristics. Qualitative trends suggest that irreversible breakdown tends to occur for long pulses or if the applied voltage is large. The precise relationship or mechanism, however, is not fully understood. A development of precise, theoretically based models would help in a proper selection of the pulse characteristics. The only theoretical simulation of resealing, to the best of our knowledge, was based on a kinetic model that treated pore closure as a one-step random process [24]. However, that treatment appears to invoke a number of approximations that can be called into question. For instance, the use of a Poisson random process is only valid provided that the events are truly independent. In actual practice, this condition is difficult to meet due to the ongoing pore interactions and the possibility for them to coalesce [25]. This is expected to become an especially important issue for high power pulses since the applied electric fields will be substantially stronger, and so should lead to the formation of a high density of pores clustered over the polar regions of each cell. Furthermore, the use of fixed, energy-independent resealing rates as in [24] is known to be an oversimplification. Self-consistent calculations of the membrane voltage are also warranted for adequately modeling the high power electroporation experiments.

In this contribution, a time-dependent numerical model based on the Smoluchowski equation [26,27] is used to simulate the pore kinetics. This equation yields the probability density function $n(r,t)$, which denotes the number of pores per unit area having radii between r and $r+dr$ at any time instant *t.* The continuous creation and destruction of pores is included, and the model keeps track of the dynamical evolution in their size. The growth, expansion, and resealing of pores is controlled by drift and diffusion in r space, and influenced by the magnitude of the transmembrane potential. This makes it necessary to incorporate the temporal variation of the cell potential. Here an equivalent circuit representation has been used for the cell to determine the transmembrane potential. Most previous studies, with the exception of a short report by Vaughan and Weaver [28], have ignored equivalent circuit aspects. As a result, the kinetic rates become time dependent, and the evolution of the biological system not only depends on the initial starting state, but also on details of the voltage wave form sequence. In short, a memory effect is naturally included in the simulation approach. Our results show that irreversible breakdown can occur if the largest pores have grown to a radii larger than a threshold value of about 20 nm by the end of the voltage pulse. It is also shown that low amplitude, long-duration electric pulses lead to the formation of a large number of small pores. These typically tend to have small radii, and will reseal upon the termination of the external field. Increases in conductance of the cell membrane, accompanying the growth in their size work to dramatically reduce the transmembrane voltage. The decay or ''discharge time constant'' is also lowered, and leads to a rapid collapse of the membrane voltage upon the termination of the applied voltage. Larger voltages, on the other hand, lead to a small number of large pores that continue to expand even in the absence of a cell potential. This suggests that high-voltage, short electric pulses could ultimately be quite efficient for the destruction of specific cells and organisms.

II. SIMULATION MODEL

In keeping with the literature [29–31], it is assumed here that two types of pores exist. The hydrophilic pores have their walls lined with water attracting heads of lipid molecules, and are conducting. These are relevant to the electroporation phenomena and lead to the large conductivity increases measured experimentally. Hydrophobic pores are nonconducting, and simply represent gaps in the lipid bilayer of the membrane. Each of the two pore types is characterized by an energy $E(r)$, which is a function of the pore radius r. In the present analysis, we have chosen to use a specific form for the pore energy in keeping with a formulation that is perhaps widely accepted and commonly used in the literature [4,19,29,32]. In this formulation, $E(r)$ represents the free energy change associated with the formation of a pore and has contributions from three factors. The surface tension of the membrane, line tension of the pore edge, and membrane capacitance collectively determine $E(r)$. Due to the contribution from the membrane capacitance, $E(r)$ acquires a dependence on the transmembrane potential $V(t)$. In the presence of a transmembrane potential $V(t)$, this energy function is given as [4,19,29,32]

$$E(r,t)=2\pi hr\sigma(\infty)[I_1(r/r_0)/I_0(r/r_0)-\pi a_p V^2 r^2, \tag{1a}$$

$$E(r,t)=2\pi\gamma r-\pi\sigma r^2+(C/r)^2-\pi a_p V^2 r^2, \tag{1b}$$

for hydrophobic and hydrophilic pores, respectively. In the above equations I_1 and I_0 are the modified Bessel functions of the zeroth and first order, respectively, h is the membrane thickness, $\sigma(\infty)$ is a constant equal to 5×10^{-2} N m^{-1}, while r_0 represents a characteristic length scale over which the properties of water change between the interface and the bulk. The value of r_0 is taken to equal 1 nm. Also, γ is the energy per unit length of the pore perimeter, while σ is the energy per unit area of the intact membrane. Typical values for the above parameters are given in Table I. The third term in Eq. (1b) represents the steric repulsion between lipid heads lining the pores [3,30], and is responsible for the in-

TABLE I. Parameters used for the theoretical model.

Parameter	Source	Value
D $(m^2\,s^{-1})$	Ref. [22]	5×10^{-14}
γ $(J\ m^{-1})$	Ref. [22]	1.8×10^{-11}
σ $(J\ m^{-2})$	Ref. [22]	10^{-3}
C $(J^{1/4}\,m)$	Ref. [33]	9.67×10^{-15}
K_w $(F\ m^{-1})$	Ref. [22]	$80\times8.85\times10^{-12}$
K_m $(F\ m^{-1})$	Ref. [22]	$2\times8.85\times10^{-12}$
h (m)	Ref. [35]	5×10^{-9}
a_p $(F\ m^{-2})$	Ref. [33]	6.9×10^{-2}
ν_c $(m^{-3}\,s^{1})$	Ref. [19]	2×10^{38}
ν_d (s^{-1})	Ref. [35]	10^{11}
r_0 (m)	Ref. [35]	1×10^{-9}
σ_0 $(N\ m^{-1})$	Ref. [35]	5×10^{-2}
R_{M0} (Ω)	Ref. [22]	1×10^{8}
R_C (Ω)	Ref. [40]	1.25×10^{4}
R_L (Ω)	Ref. [40]	50
C_M (nF)	Ref. [22]	9.6
C_S (nF)	Ref. [41]	0.02

crease in pore free energy with shrinking radius. The value of C in Eq. (1b) was chosen to be 9.67×10^{-15} $J^{1/4}\,m$ in keeping with the reports by Neu and Krassowska [30] as it yields values close to those measured by Glaser *et al.* [32]. The last term in Eq. (1b) represents the capacitive contribution to the energy in the presence of a transmembrane potential V. The coefficient a_p is a property of the membrane and its aqueous environment. In the simples continuum approximation [32], it is expressed in terms of the membrane thickness h and the permittivities ϵ_w and ϵ_m of water and the membrane, respectively, as $a_p=(\epsilon_w=\epsilon_m)/[2h]$. Values of these various parameters are relatively well known, and have been given in Table I.

It might be mentioned that other models have been proposed as well that take into account different factors in the pore energy calculation. For instance, formulations based on the role of osmotic pressure [18], electrocompression of the lipid bilayer [33], interaction with membrane cytoskeleton [34], and more recently cellular deformation [35] exist. While the expression for $E(r)$ would change somewhat on the basis of the alternative theories, the basic trends and qualitative physical behavior would remain unaltered. A careful comparative analysis of the various formulations will be carried out elsewhere. Also, the surface tension has been assumed to be a constant in the present treatment. In practice, σ value can change depending on the osmotic pressure, or with perforation in a finite membrane upon stretching. For example, a simple heuristic model has recently been used to describe such changes [35], and an electrostatic treatment has also been proposed [36]. The primary effect of such variations in σ, as shown in Ref. [35], would be the creation of an additional local minima in the pore energy function. The value of the pore radius corresponding to this minima would be larger than that corresponding to the unstable minima. The net change from the standpoint of electroporation would be that instead of expanding continually beyond the unstable maxima, the pores would become quite large and ultimately stabilize at this high radial value. In principle though, the possibility of creating cell membranes with very large pores potentially leading to cell destruction over time would remain. Hence most consequences and the qualitative reasoning presented here would hold despite the assumption of a fixed σ parameter.

The energy function $E(r)$ is important to the pore dynamics for several reasons. First, it determines the ''drift flux'' for pores in r space, and therefore governs the growth or contraction of pores at any given radius ''r.'' A positive $E(r)$ slope signifies a driving force toward a smaller radius, while a negative slope forces the growth and expansion of pores in r space. This makes the gradient of $E(r)$ an important parameter in the Smoluchowski equation for the pore kinetics. Second, the $E(r)$ profile contains local maxima and minima in r space, which are dependent on the applied voltage. In general, the presence of a membrane voltage reduces the maxima, and can even quell the energy barrier completely beyond a critical voltage value. In the latter situation, pores would tend to grow without bound, and lead to cell rupture. Not only is the presence or absence of a confining barrier potential dependent on the $E(r)$ profile, but the drift velocity in r space is also controlled by the shape of $E(r)$. This is particularly relevant to transient voltage pulses, since stability depends upon whether the pores are able to drift past the barrier *maxima within the duration of the applied voltage pulse*. Finally, the energy $E(r)$ dictates the rate of formation of new pores as a function of r.

As in previous treatments, it is assumed here that the formation of pores is a two-step process. All pores are initially created as hydrophobic/nonconducting at a rate $S(r)$ per unit area of the membrane, during every time interval dt. This rate is given as

$$S(r)=\{(\nu_c h)/(k_B T)\}[dE(r)/dr]\exp[-E(r)/(k_B T)]dr\,dt, \tag{2}$$

where ν_c is an attempted rate density [19], $E(r)$ is the energy for hydrophobic pores, T is the operating temperature, and k_B is the Boltzmann constant. This assumes that the use of a kinetic collisional theory remains valid for nongaseous phases as well. This is easily justified given that kinetic, collisional approaches (and Langevin equations to include memory effects) have been used for a variety of problems in condensed matter physics [37,38]. If a conducting pore is created with a radius $r>r^*$, it spontaneously changes its configuration and transforms into a conducting, hydrophilic pore. All conducting pores then survive as long as their radii remain larger than r^*. Destruction of a conducting pore occurs only if it drifts or diffuses in r space to a value below r^*. Due to the exponential term in Eq. (2), most pores are created with very small radii. It is only under the influence of a suitably sloped $E(r)$ curve, such as that resulting from an applied voltage, that the created pores would begin to drift and diffuse toward higher radii.

The Smoluchowski equation that governs the pore dynamics is given in terms of the pore density distribution function $n(r,t)$ as

$$\partial n(r,t)/\partial t-\{D/k_B T]\}[\partial E(r)/\partial r]-D\partial^2 n(r,t)/\partial r^2=S(r), \tag{3}$$

where $S(r)$ is the source term as given in Eq. (2), while D is the pore diffusion constant given in Table I. The Smoluchowski approach was originally used in the treatment of Brownian motion [27], in which the fluid molecules are in a state of constant flux. The process of diffusion represents a ''random walk'' of the pore radius in r space. Physically, this is brought about by fluctuations in the radius in response to water molecules and other species constantly entering and leaving the pores. The total number of pores $N(t)$ is easily expressed in terms of the probability density function $n(r,t)$ as $N(t)=\int_0^\infty n(r,t)dr$. Similarly, the average pore radius $\langle r(t)\rangle$ at any time instant can be expressed as $\langle r(t)\rangle = [\int_0^\infty rn(r,t)dr]/[\int_0^\infty n(r,t)dr]$.

Numerical simulations of the dynamic pore distribution were carried out here by implementing a time-domain, finite difference discretization of the governing Smoluchowski equation. An upperbound $r_{\max}$ of 50 Å was set on the pore radius, and this entire r space was uniformly divided into 1000 segments to yield a constant grid spacing dr of 0.05 Å. This choice of the boundary on the r space was guided by two factors. First, the set limit had to be much larger than the critical radius r_c at which the energy function $E(r)$ has a local maxima. This ensured that the region of r space well beyond the potential barrier was adequately included. As already discussed, the pores can be expected to continually grow without bound once their radius exceeds r_c. So to probe instabilities leading to irreversible pore rapture, it is necessary for $r_{\max}$ to exceed r_c at zero transmembrane potential. Next, from previous work it is known that the equilibrium values of the pore radii are on the order of 0.8 Å . Hence the chosen limit $r_{\max}$ had to substantially exceed this equilibrium value to allow for the adequate simulation of nonequilibrium phenomena. Since the governing equation (3) is a second order partial differential equation, two suitable boundary conditions had to be imposed. Here, a ''reflecting boundary'' was assigned at $r=r_{\max}$, which was implemented by setting the pore flux to zero at $r=r_{\max}$. Mathematically, this amounts to a Neumann conditionof the form $[dn(r,t)/dr]|_{r=r\,\max} = -[dE(r,t)/dr][n/(k_BT)]_{r=r\,\max}$. At the other end, absorbing boundary conditions were implemented by setting $n(0,t)=0$. The time step dt in these simulations was chosen to be much smaller than the fluctuation rate ν_d, which represents the fastest time constant in the system [32]. Specifically, $dt=10^{-12}$ s was used. As an initial condition prior to the application of an external voltage, the pore density was taken to be zero at all the grid points. With zero applied voltage, the function $n(r)$ is then expected to reach a finite steady state, with an average pore size of about 0.8 Å . This is a simple validity check on the numerical scheme implemented here, and was carried out in this work as discussed in Sec. III.

The voltage $V(t)$ was taken to have the exact time-dependent shape corresponding to the external pulsed wave form. The wave form was taken to have a basic rectangular shape with exponentially rising and falling components. The rise and fall times were chosen to be 2 ns. For the purposes of calculating the transmembrane potential, a lumped equivalent circuit as shown in Fig. 1 was employed. The use of such a lumped circuit model for the cell perhaps requires some justification, especially in light of a recent report on the use of distributed transmission networks for cellular modeling [39]. The lumped approach is justified as long as the distributed effects associated with the wave nature of electrical signals can be ignored. Typically, a distributed model is invoked to take into account the finite time ΔT required for the imposed signals, moving at the speed of light, to propagate along their path. If the time interval ΔT is comparable to or larger than the time period T of the signal, then distributed effects become necessary. Here, for the simulation of a single cell, the largest distance corresponds to the cellular diameter. Assuming a value on the higher side of about 680 μm, and taking a propagation velocity of 3×10^7 ms^{-1} (i.e., a factor of 10 lower than the light speed in a vacuum), one obtains $\Delta T=2.26\times10^{-11}$ s. This translates into a frequency in excess of 40 GHz. Since the frequency of the applied signals or their dominant Fourier transform components are never as large, it seems fairly reasonable to use a lumped circuit model. It must be pointed out though, that in the present work, a circuit representation for the inner nucleus has not been included. This essentially ignores the role of the nucleus. The present model is therefore valid as long as the nuclear dimensions are much smaller than the cell size, or if its time constants are sufficiently different from those of the membrane and cellular processes.

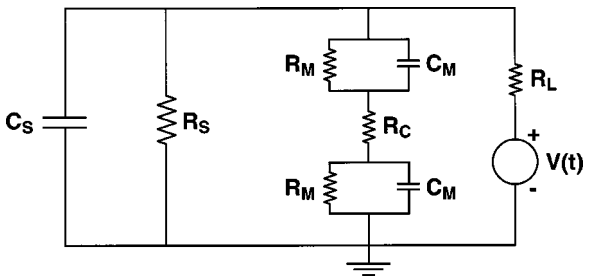

FIG. 1. Lumped equivalent-circuit diagram of a cell used for computing the transmembrane potential. The resting transmembrane potential was set to zero.

The equivalent circuit of Fig. 1 displays a resistance R_M and capacitance C_M associated with the cell membrane, an R_C element representing the resistance of the cell fluid, and a R_L element representing the external circuit resistance, which includes the contacts and wires. Elements R_S and C_S are the resistance and capacitances of the cell suspension, respectively. The membrane resistance R_M represents the conductivity of the cell membrane, which is typically a voltage controlled parameter. Physically, as electroporation begins within a cell, the ionic flow through the newly created aqueous pores increases. This leads to enhanced conductivity, and can macroscopically be described in terms of a voltage controlled conductance. Since the resistance is inversely proportional to the pore size, R_M has been modeled here as a time varying function of the effective pore area. Quantitatively, this translates into the following equation for $R_M(t)$:

$$R_M(t)=R_{M0}[\Sigma A_p\{V=0,t\rightarrow\infty\}]/[\Sigma A_p\{V(t),t\}]. \quad (4)$$

In the above equation, R_{M0} is the initial value of the membrane resistance, under steady-state conditions for zero voltage. The parameter A_p is the area of all the pores, which is dependent on the time and the applied voltage. Equation (4) implies that each pore does not have the same size, but is

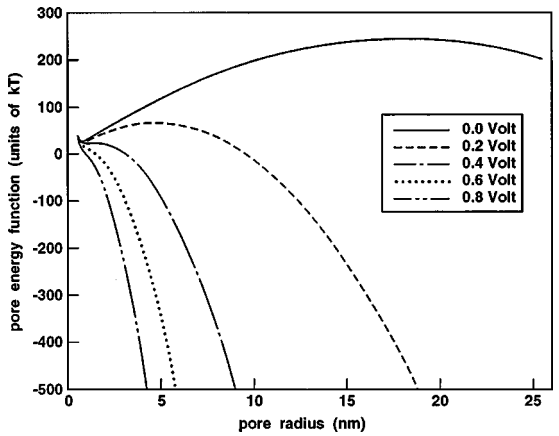

FIG. 2. Energy for hydrophilic pores, as a function of the pore radius for different values of the transmembrane potential.

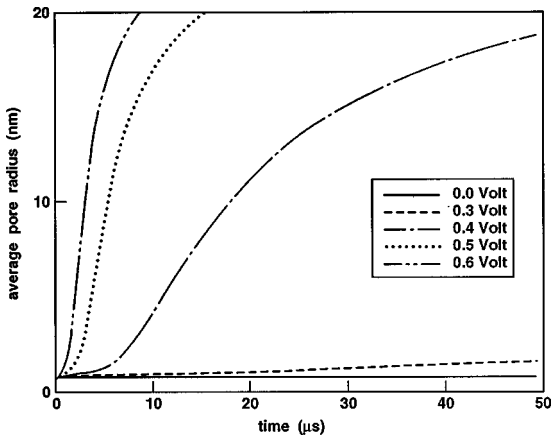

FIG. 3. The temporal evolution of the average pore radius $\langle r(t)\rangle$ in response to various values of the transmembrane potential.

governed by the distribution function $n(r,t)$ for pores with radii lying between r and $r+dr$. Since $n(r,t)$ is obtained numerically through a solution to the equation, the area can be ascertained at each time step. The numerator on the right side of Eq. (4) can be obtained through numerical simulations for zero applied voltage, carried out for long times. The value of R_{M0} was chosen to be 100 MΩ in keeping with previous reports [22]. Finally, since the area is obtained dynamically, the aqueous fractional area $F_W(t)$, which yields the ratio of pores to the total cell area, can be computed easily as

$$F_W(t)=\left[\int_0^\infty \pi r^2 n(r,t)dr\right]/[\pi R^2], \tag{5}$$

where R is the radius of the cell.

III. RESULTS AND DISCUSSION

The energy $E(r)$ for hydrophilic pores, as a function of the pore radius for different values of the transmembrane potential at 300 K, is shown in Fig. 2. Since the evolution dynamics of the pores is controlled by this parameter, a discussion of $E(r)$ brings out trends in dynamical growth as a function of the pore size. For zero applied voltage, a local minima in the pore energy is predicted at about 0.8 nm. This corresponds to the average or most likely pore size, under steady-state equilibrium conditions. Figure 2 also predicts a local maxima for the zero voltage case, at a pore radius of about 18 nm. From the shape of the energy function, it becomes clear that all pores having radii less than 18 nm would tend to experience a drift flux in r space toward smaller values. Physically, the monotonic increase in pore energy below 18 nm would force the pores in the system to shrink in size and dynamically approach the 0.8 nm radius. Pores with radii exceeding this threshold, however, would drift toward larger values and expand without bound in an uncontrolled fashion. Irreversible breakdown and cell rupture would therefore be the expected result, if pores could reach beyond the stability threshold radius $r_{\rm crit}$ of 18 nm. At a 0.2 V transmembrane potential, a dramatic shift in both the peak energy and the radius of the local maxima is predicted. The critical radius for stability reduces to about 5.8 nm, and so the probability that some fraction of the pores will exceed the stability threshold correspondingly increases. The local minima is not perturbed, and so the expected radius under steady state equilibrium conditions still remains roughly at 0.8 nm. The important point is that a potential barrier exists for the 0.2 V voltage, and so irrespective of the pulse duration, the cells are not expected to undergo irreversible breakdown. For 0.4 V across the cellular membrane, the maxima is virtually eliminated. This therefore represents the minimum voltage that would lead to cellular breakdown, provided the voltage was applied long enough to enable the pores to grow past the 18 nm critical threshold. Since this voltage would apply across both the upper and lower segments of a spherical cell, this corresponds to a total voltage of 0.8 V across the entire cell. For a pulse voltage, on the other hand, a breakdown need not necessarily occur for the 0.4 V transmembrane potential, if the time duration of the pulse were short. Under a short duration scenario, pores would expand but not have sufficient time to increase beyond $r_{\rm crit}$. As a result, once the pulsed voltage reverted back to a zero magnitude, the pores would all begin to shrink and recover in size to the 0.8 nm level. Similarly, at the higher voltages of 0.6 and 0.8 V, the local maxima is not seen, and the pores can potentially expand irreversibly without bound. However, here again in the context of a pulsed voltage, membrane rupture can only take place provided the pore radius has expanded beyond the $r_{\rm crit}$ threshold over the duration of the pulse. If instead the pulse is terminated before this critical expansion can take place, then the cell should recover and the pores should slowly disappear over time. Based on the above logic, it also becomes apparent that there should be a critical ''on-time'' requirement for cell destruction, and that its magnitude should decrease with applied voltage. At higher voltages, the slope of $E(r)$ is more strongly negative, which is indicative of faster pore drift in r space. Hence the pulse would not need to be on for as long a time before driving the pore radius beyond $r_{\rm crit}$. A voltage-dependent characteristic time can therefore be expected for cellular breakdown under pulsed power conditions.

Next, time-dependent simulations were carried out based on the Smoluchowski approach to probe the dynamics. Figure 3 shows the temporal evolution of the average pore radius $\langle r(t)\rangle$ in response to various values of the transmembrane potential. The initial condition assumed zero pores,

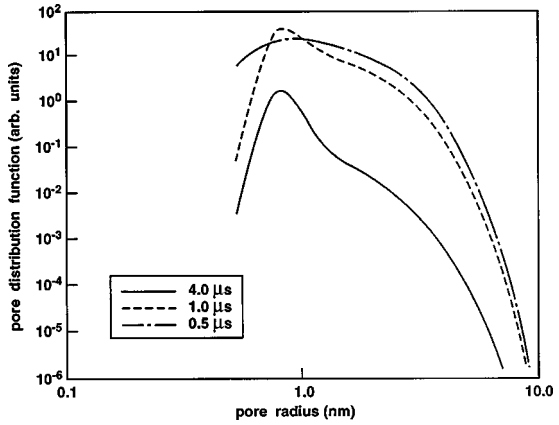

FIG. 4. Results of the pore distribution function at three time instants in response to a 0.8 V, 0.5 μs applied voltage pulse. Irreversible damage is not predicted.

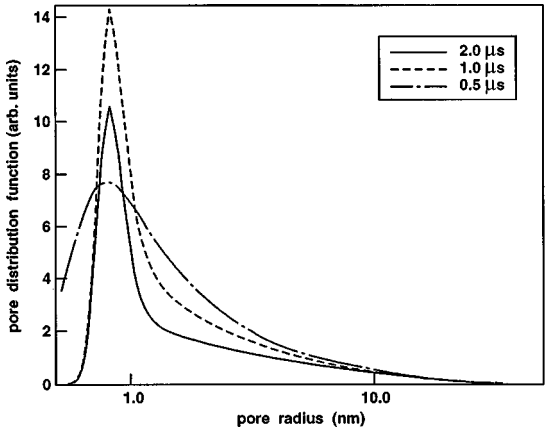

FIG. 5. Results of the pore distribution function at three time instants for a 1.2 V, 0.5 μs applied voltage pulse. Complete recovery is not predicted.

and so the assigned value for the radius was zero at the start. For a zero volt voltage, a steady state is seen to be reached fairly quickly within 1 μs. The predicted steady state value is about 0.8 Å , in keeping with the local minima of Fig. 2. This result thus validates the simulation scheme and its numerical implementation. For nonzero membrane voltages of 0.33, 0.4, 0.5, and 0.6 V, the pores are predicted to continually expand in size and the average radii to increase with time. The results clearly reveal that the time required to reach the 20 nm threshold depends very nonlinearly on the applied voltage. For example, times on the order of 5 μs are predicted for 0.4 V, while this duration reduces dramatically to 1.5 and 0.8 μs at voltages of 0.5 and 0.6 V. It must be pointed out that the time durations of Fig. 3 are only indicative of rough upperbounds. This overestimation results because breakdown is not controlled by the average size of the *entire population*, but rather by the presence of a few pores with radii exceeding r_{crit}. Thus in actual practice, the pulse durations required would be smaller, since they would require only a few pores from the distribution spanning the entire r space to cross the threshold radius.

In order to better understand the individual pore dynamics and temporal variations in the overall collection, results of the pore distribution function $n(r,t)$ for two voltage input pulses are presented and discussed next. In Fig. 4, three snapshots of the distributions at the observation times of 0.5, 1.0, and 4.0 μs are shown for a 0.8 V pulse across the membrane having a 0.5 μs duration. The distribution $n(r,\ t=0.5\ \mu\mathrm{s})$ immediately following the termination of the voltage has the broadest profile and the highest values beyond a 1 nm pore radius. Hence starting from a zero value at the initial time, the 0.8 V membrane pulse is predicted to cause a broad increase in the pore population, with a finite nonzero distribution spanning well beyond the 0.8 nm equilibrium radius. However, the result also indicates that for times beyond 0.5 μs, the pores would continually begin to shrink in size, and the distribution would shift to lower values of the radius. The 1.0 μs snapshot reveals a peak at about 0.8 nm, which is roughly the equilibrium value. Finally, at 4 μs, the pores have essentially decreased in number and clustered more around the 0.8 nm level. The obvious inference is that a 0.8 V pulse having a duration of only 0.5 μs would be insufficient to cause irreversible damage to the cell.

The results for a 1.2 V pulse having the same 0.5 μs duration, however, are predicted to be substantially different. Shown in Fig. 5 are three snapshots of the pore distribution at times of 0.5, 1.0, and 2.0 μs. As compared to Fig. 4, the distribution in Fig. 5 is a few orders of magnitude higher. This is simply the result of a much larger generation rate that depends exponentially on the membrane voltage. For this situation, complete recovery is not predicted. As in Fig. 4, the 0.5 μs distribution has the broadest shape. After termination of the voltage pulse, all pores having radii below the 20 nm local maxima begin to shrink. This is primarily the result of a positive $E(r)$ slope, which provides a net drift in r space toward lower values. The peak is seen to have increased appreciably at 1.0 μs and is located at a radius of about 8 nm. At the later time of 2.0 μs, the peak still appears near the equilibrium level, but has a reduced magnitude. These collective results are consistent with a dynamic shrinkage of pores below the 18 nm threshold. However, for radii beyond 18 nm, the curves of Fig. 5 do not exhibit any appreciable change with time. Instead, the pores are predicted to remain without recovery. Given magnitudes that are well above 1000, it is clear that this irreversible process is likely to cause permanent damage due to the gradual and continuous transport of ions and cell matter through these large numbers of open pores.

The above differences in evolution for pores below and above the 18 nm threshold radius r_{crit} is probed further in Fig. 6. The temporal dynamics of the entire pore population below 18 nm is plotted, together with the populations above r_{crit}. A 1.6 V, 0.5 μs pulse was assumed. The population of pores having radii below r_{crit} immediately shows a rapid increase that continues to about 0.3 μs. The growth rate relatively slows between the 0.3 and 0.5 μs interval, as some of the bigger pores begin crossing the R_{crit} threshold. As a result, the corresponding population of the $r>r_{\mathrm{crit}}$ group starts to increase dramatically at about 0.3 μs. Following the termination of the voltage pulse at 0.5 μs, the population of the group with the smaller radii begins to decrease. However, the numbers of the $r>r_{\mathrm{crit}}$ group exhibit a continued increase beyond 0.5 μs. This simulation provides a clear indication of irreversible breakdown and the nonrecovery of the cell

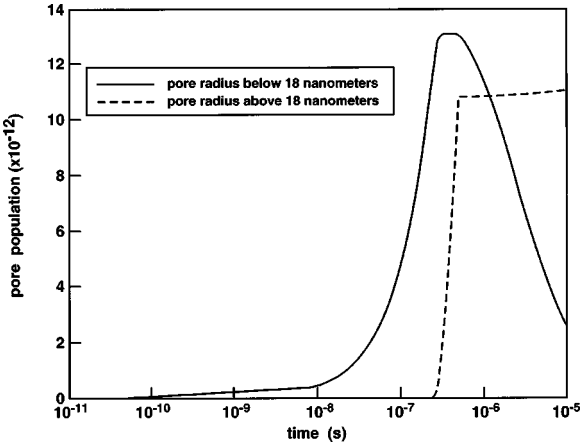

FIG. 6. Temporal evolution of the pore populations with radii above and below 18 nm response to a 1.6 V, 0.5 μs applied voltage pulse.

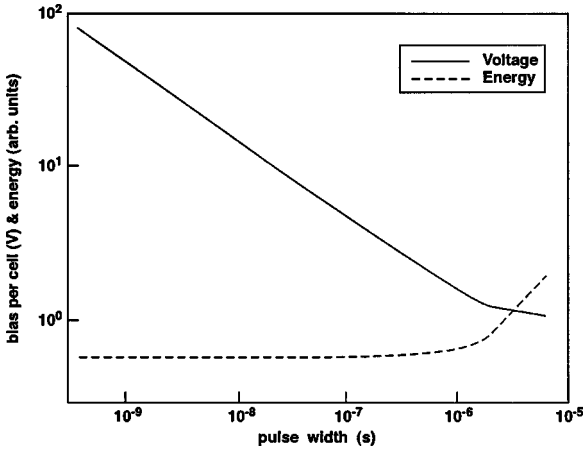

FIG. 7. Calculations of the voltage and energy versus the minimum pulse width necessary to initiate irreversible breakdown.

membrane following the 1.6 V pulse.

The above results quantitatively shown the important role of both the applied voltage and the pulse duration in affecting irreversible breakdown. However, in order to validate this model further, it is important to make direct comparisons between the model predictions and actual observable quantities. Unfortunately, neither pores not their distributions can be measured directly, and so direct comparisons cannot be made. Here, for purposes of making direct comparisons, we examine the relationship between applied voltage (and hence the input energy) and the pulse width necessary for irreversible breakdown. As a first step, such a relationship would help in providing useful guidelines on the pulse characteristics for pulsed power applications. In addition, carefully comparing predicted trends between the voltage and pulse widths with experimental observations would yield a direct assessment of the present model. The pulse width necessary for bringing about irreversible breakdown at a given applied voltage can roughly be estimated by focusing on the drift term of the Smoluchowski equation. The rate of change in the pore radius (i.e., the velocity term that controls the pore growth) is given as $dr/dt=[dE(r)/dr]*\{D/[k_BT]\}$. Using the expression for the hydrophilic pore energy, and ignoring the steric repulsion term, one obtains

$$dr/dt=\{D/[k_BT]\}[2\pi\gamma-2\pi\sigma r-2\pi a_pV^2r]. \quad (6)$$

Clearly, for irreversible breakdown, the pore radius has to grow in response to the applied voltage from a value of $r_{\min}=0.8$ mn (i.e., roughly the equilibrium level) to at least $r_{\rm crit}$ while the pulse is on. Hence the minimum pulse width $t_{\rm pulse}$ required for the breakdown threshold to be reached can be computed by integrating Eq. (5) between the limits of $r_{\rm crit}$ and $r_{\min}$. The result is straightforward, and yields the following relationship:

$$t_{\rm pulse}=\{[k_BT]/D\}[2\pi\sigma+2\pi a_pV^2]^{-1} \times\{[-\gamma+(\sigma+a_pV^2)r_{\rm crit}]/[-\gamma(\sigma+a_pV^2)r_{\min}]\}. \quad (7)$$

Based on the above expression, the values of minimum pulse width can be computed as a function of the transmembrane potential V. The results are shown in Fig. 7. The total input energy, which is proportional to $V^2t_{\rm pulse}$, is also given. The pulse widths range from about 10^{-5} s to slightly less than 1 ns and correspond to voltage variations lying between 1.1 and 70 V. The range of the pulse widths matches the typical experimental time scales that have been used recently and reported by one of us [13]. Hence the model gives very good agreement. The voltage trend predicted here also matches the observations reported in Ref. [13]. For example, a similar two-region curve is predicted here, with a slower voltage for longer pulses beyond 1 μs, and a sharper rise for the lower pulse durations. The change in slope is associated with the requirement of a minimum threshold voltage for bringing about irreversible damage. The energy curve predicts a sharp decrease as the pulse widths are reduced from beyond the microsecond range. A similar trend was observed in Ref. [13]. Technologically, in terms of the overall system efficiency, this result makes a compelling case for the use of pulse widths that have durations lower than 1 μs. However, a saturating effect is predicted below the submicrosecond range. This again is in keeping with a report on *E. coli* studies [13]. This simple model therefore suggests that there would be no compelling reasons for reducing the pulse widths below the 0.1 μs level. However, it must be pointed out that the present model applies only to the electroporation process at the lipid bilayer of the cellular membrane. However, other considerations such as the dynamics of the nuclear membrane or other processes may favor the use of lower pulse widths.

A final comment concerns the role of dissipation in the biological system. The result presented above did not include the circuit aspects and hence did not account for the dissipative energy losses within the various equivalent resistors. For self-consistency, and to probe the effects of equivalent circuit parameters, calculations for the voltage-dependent pulse width were carried out by using the circuit model of Fig. 1. In this situation, the expansion and growth of pores would not be limited to the duration of the applied pulse, but could also occur during the ''OFF'' state as long as the membrane capacitor voltage was above its zero value. This voltage decay time, as well as the initial charging times, would both depend on the time constants for the equivalent circuit. The role of circuit parameters in this regard is demonstrated in Fig. 8, which shows the time dependence of the transmembrane potential in response to a 2 V, 0.5 μs voltage pulse.

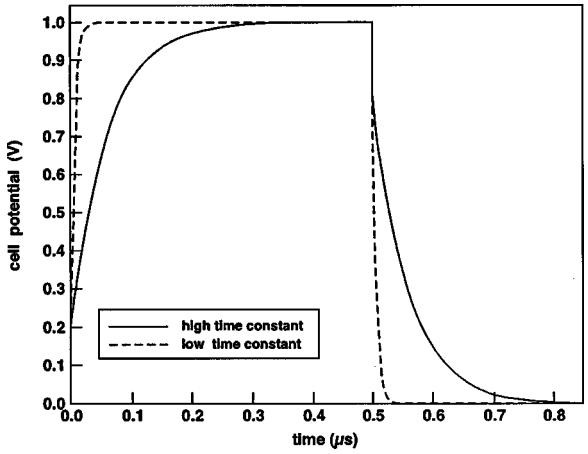

FIG. 8. Time dependence of the transmembrane potential in response to an applied 2 V, 0.5 μs voltage pulse for two different internal circuit time constants.

Simulations were performed based on the values given in Table I. Two different time constants (i.e., $C_M R_c$ values) were used to bring out differences in the response. Based on Fig. 8, the rise and fall times for the two cases are seen to be roughly 0.018 and 0.2 μs, respectively. These results bring out a very clear implication for short voltage pulses. For instance, with a slow internal time constant, the full voltage would not be applied across the individual cell membrane if pulse durations were less than 0.2 μs in this case. Due to the lower value of the actual cell potential, a higher threshold would be necessary to cause the same destructive effect for smaller pulse widths. The demands on the expended energy would also increase as the pulse durations shrunk toward the submicrosecond regime.

Results for the voltage threshold at a given pulse width, including circuit effects, obtained from the use of the Smoluchowski drift term are show in Fig. 9. Time constants of 20 ns and 2 μs were used as typically representing the values for microbes and mammalian cells, respectively. These values can easily be obtained from typical parameters such as the cell resistivity, capacitance, and cell area [40]. The figure shows both the requisite applied voltage V and the corresponding energy (i.e., $V^2 t_{\text{pulse}}$) as a function of the pulse width t_{pulse}. As compared to Fig. 7, two main effects are

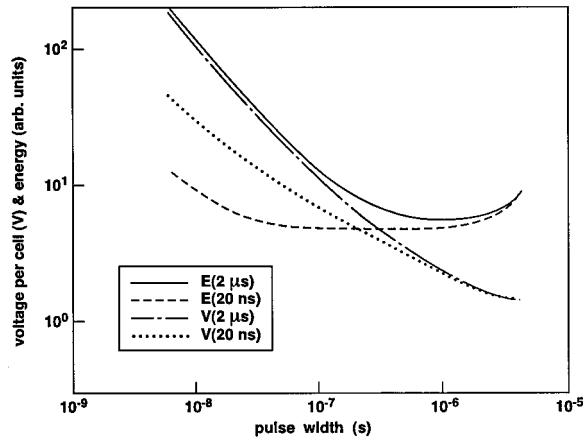

FIG. 9. Calculations of the voltage and energy versus minimum pulse width for irreversible breakdown with circuit effects taken into account.

immediately obvious. First, both the voltage and the energy input are substantially larger with circuit effects taken into account. Physically, this conclusion is in keeping with the additional dissipation included in the system. Second, the shape of the energy function changes and exhibits a local minima. The location of this minima is dependent on the charging time parameter. For example, for a 20 ns value, a relatively broad minima is predicted. However, the 2 μs value has a much narrower regime centered around 0.75 μs. Furthermore, the asymptotic behavior at the low pulse widths shown in Fig. 7 has now disappeared in Fig. 9. The main conclusions that can be drawn from the above are the following:

(i) There will exist a local minima in the energy versus pulse width curve. From a practical standpoint, this corresponds to an optimal pulse width setting for bringing about irreversible damage to biological cells.

(ii) The precise location of this optimal pulse width and the energy input necessary will depend on the details of the cellular species and the internal time constants. In general, for cells having a smaller time constant, a better system efficiency would result from the use of such a pulsed power approach.

(iii) A decrease in the internal RC time constant, will shift the optimal operating point to lower pulse widths.

(iv) Finally, it is possible then to obtain somewhat different energy-pulse width (E-P) characteristics depending on the organism under study. This prediction is in excellent agreement with a previous experimental report [13] that clearly showed varying E-P shapes.

IV. SUMMARY AND CONCLUSIONS

A model analysis of electroporation in biological cells has been carried out based on the Smoluchowski equation. One of the objectives was to obtain predictions and a qualitative understanding of the cellular response to short, electric pulses by taking account of the growth and resealing dynamics. The physical processes of pore generation, drift, and diffusion in r space were all comprehensively included. The free energy of pore formation was shown to be important, and have a role in the following aspects:

(i) Determination of the steady state pore distributions and average pore size.

(ii) Influence on the generation rate, which also depends on the transmembrane potential.

(iii) The existence of a natural stability region in r space. It was shown that pores with radii less than a critical threshold would recover (or heal) and not lead to irreversible breakdown.

(iv) The existence of a threshold voltage for a given pulse width based on the drift in r space controlled by the energy $E(r)$.

It was shown via simulations that the application of large voltages along may not be sufficient to cause irreversible breakdown, if the time duration is short. It has been argued here that the failure to cause irreversible damage at small pulse widths can be attributed to the time inadequacy for the pores to grow and expand beyond the critical threshold radius. Also, implicit is a memory effect for the system. It follows from the present discussion that if a subsequent volt-

age pulse were to be applied before the pores had a chance to fully recover to their equilibrium values, then a much shorter time duration would be required for irreversible failure.

The transmembrane potential for irreversible breakdown for quasistatic pulses has been shown to be about 0.5 V, which leads to a total cell potential of 1.0 V. This is in keeping with previous reports in the literature. It was also shown that irreversible breakdown would lead to the formation of a few large pores, while a large number of smaller pores would result in the case of reversible breakdown. Finally, the pulse width dependence of the applied voltage was obtained based on the growth of pores to the critical radius. In the absence of dissipation, the energy input necessary was shown to reduce with decreasing pulse width and reach a limiting value. However, with circuit effects taken into account, a local minima in the pulse dependent energy function is predicted. This is in keeping with some previously published experimental reports, and thus provides indirect validation of present model. It has also been shown that an optimal pulse width in the submicrosecond regime is likely to exist for irreversible damage to biological cells. This confirms an inherent utility for ultrashort, pulsed-power sources. More careful calculations to include mass transport, variable surface tension, cellular deformations and the effects on circuit equivalent circuit parameters will have to be carried out for a better representation and understanding of the actual biological system.

ACKNOWLEDGMENTS

The authors would like to thank J. Weaver (MIT) and W. Krassowska (Duke University) for useful discussions. This work was sponsored in part by the U.S. Air Force Office of Scientific Research. Support from Old Dominion University is also gratefully acknowledged.

[1] R. Stampfli, An. Acad. Brasil. Ciens. **30**, 57 (1958).
[2] T. Y. Tsongi, Biophys. J. **60**, 297 (1991).
[3] J. C. Weaver and Yu. A. Chizmadzhev, Bioelectrochem. Bioenerg. **41**, 135 (1996).
[4] I. G. Abidor, V. B. Arakelyan, L. V. Chernomordik, Y. A. Chizmadzhev, V. F. Pastushenko, and M. R. Tarasevich, Bioelectrochem. Bioenerg. **6**, 37 (1979).
[5] G. A. Hoffmann, S. B. Dev, and G. S. Nanda, IEEE Trans. Biomed. Eng. **46**, 752 (1999).
[6] D. C. Chang, B. M. Chassy, J. A. Saunders, and A. E. Sowers, in *Guide to Electroporation and Electrofusion* (Academic Press, New York, 1992).
[7] E. Neumann, E. Sowers, and C. A. Jordan, in *Electroporation and Electrofusion in Cell Biology* (Plenum, New York, 1989).
[8] S. Orlowski and L. M. Mir, Biochim. Biophys. Acta **1154**, 51 (1993).
[9] J. C. Weaver, J. Cell. Biochem. **51**, 426 (1993).
[10] A. J. H. Sale and W. A. Hamilton, Biochim. Biophys. Acta **148**, 781 (1967).
[11] H. Huelsheger, J. Potel, and E. G. Niemann, Radiat. Environ. Biophys. **20**, 53 (1981).
[12] K. H. Schoenbach, R. W. Alden, III, and T. J. Fox (unpublished).
[13] K. H. Schoenbach, F. E. Peterkin, R. W. Alden, and S. J. Beebe, IEEE Trans. Plasma Sci. **25**, 284 (1997).
[14] R. Benz and U. Zimmermann, Biochim. Biophys. Acta **597**, 637 (1980).
[15] A. Barnett and J. C. Weaver, Bioelectrochem. Bioenerg. **25**, 163 (1991).
[16] Yu. A. Chhizmadzhev, V. B. Arakelyan, and V. F. Pastushenko, Bioelectrochem. Bioenerg. **6**, 63 (1979).
[17] J. D. Lister, Phys. Lett. **53A**, 193 (1975).
[18] C. Taupin, M. Dvolaitzky, and C. Sauterey, Biochemistry **14**, 4771 (1975).
[19] J. C. Weaver and R. A. Mintzer, Phys. Lett. **86A**, 57 (1981).
[20] M. Hibino, M. Shigemori, H. Itoh, K. Nagyama, and K. Kinosita, Biophys. J. **59**, 209 (1991).
[21] C. Wilhelm, M. Winterhalter, U. Zimmermann, and R. Benz, Biophys. J. **64**, 121 (1993).
[22] S. A. Freeman, M. A. Wang, and J. C. Weaver, Biophys. J. **67**, 42 (1994).
[23] I. P. Sugar, in *Electroporation and Electrofusion in Cell Biology*, edited by E. Neumann, E. Sowers, and C. A. Jordan (Plenum, New York, 1989), pp. 97–110.
[24] G. Saulis, Biophys. J. **73**, 1299 (1997).
[25] I. P. Sugar, W. Forster, and E. Neumann, Biophys. Chem. **26**, 321 (1987).
[26] V. F. Pastushenko, Yu. A. Chhizmadzhev, and V. B. Arakelyan, Bioelectrochem. Bioenerg. **6**, 53 (1979).
[27] For example, see R. K. Pathria, *Statistical Mechanics* (Pergamon, Oxford, 1972), pp. 451–455.
[28] T. Vaughan and J. C. Weaver, in *Electricity and Magnetism in Biology and Medicine*, edited by A. Bersani (Kluwer Academic, New York, 1999), p. 433.
[29] J. C. Weaver, Ann. (N.Y.) Acad. Sci. **720**, 141 (1994).
[30] J. C. Neu and W. Krassowska, Phys. Rev. E **59**, 3471 (1999).
[31] J. Teissie and M. P. Rols, Ann. (N.Y.) Acad. Sci. **720**, 98 (1994).
[32] R. W. Glaser, S. L. Leikin, L. V. Chernomordik, V. F. Pastushenko, and A. I. Sokirko, Biochim. Biophys. Acta **940**, 275 (1988).
[33] I. P. Sugar, Biochim. Biophys. Acta **556**, 72 (1979).
[34] W. Sung and P. J. Park, Biophys. J. **73**, 1797 (1997).
[35] H. Isambert, Phys. Rev. Lett. **80**, 3404 (1998).
[36] M. Winterhalter and W. Helfrich, Phys. Rev. A **36**, 5874 (1987).
[37] C. Jacoboni and P. Lugli, in *Monte Carlo Method for Semiconductor Device Simulation* (Springer-Verlag, Berlin, 1989).
[38] A. M. Kriman, D. K. Ferry, M. J. Kann, and R. P. Joshi, Comput. Phys. Commun. **67**, 119 (1991).
[39] T. R. Gowrishankar (private communication).
[40] K. S. Cole, Trans. Faraday Soc. **23**, 966 (1937).
[41] H. P. Schwan, in *Interactions Between Electromagnetic Fields and Cells*, edited by A. Chiabrera, C. Nicolini, and H. P. Schwan (Pergamon, New York, 1985), p. 75.